Non-invasive anatomic and functional imaging of vascular inflammation and unstable plaque

Camici, P G ; Rimoldi, O E ; Gaemperli, O ; Libby, P

DOI: https://doi.org/10.1093/eurheartj/ehs067

European Heart Journal (2012) **33**, 1309–1317
doi:10.1093/eurheartj/ehs067

REVIEW

Imaging

Non-invasive anatomic and functional imaging of vascular inflammation and unstable plaque

Paolo G. Camici[1]*, Ornella E. Rimoldi[2], Oliver Gaemperli[3], and Peter Libby[4]

[1]Vita-Salute University and Scientific Institute San Raffaele, Via Olgettina 60, Milan 20132, Italy; [2]CNR, IBFM, Milan, Italy; [3]Interventional Cardiology and Cardiac Imaging, Cardiovascular Center, University Hospital Zurich, Zurich, Switzerland; and [4]Division of Cardiovascular Medicine, Department of Medicine, Brigham and Women's Hospital, Harvard Medical School, Boston, MA, USA

Received 4 January 2012; revised 9 February 2012; accepted 28 February 2012; online publish-ahead-of-print 16 April 2012

Over the last several decades, basic cardiovascular research has significantly enhanced our understanding of pathobiological processes leading to formation, progression, and complications of atherosclerotic plaques. By harnessing these advances in cardiovascular biology, imaging has advanced beyond its traditional anatomical domains to a tool that permits probing of particular molecular structures to image cellular behaviour and metabolic pathways involved in atherosclerosis. From the nascent atherosclerotic plaque to the death of inflammatory cells, several potential molecular and micro-anatomical targets for imaging with particular selective imaging probes and with a variety of imaging modalities have emerged from preclinical and animal investigations. Yet, substantive barriers stand between experimental use and wide clinical application of these novel imaging strategies. Each of the imaging modalities described herein faces hurdles—for example, sensitivity, resolution, radiation exposure, reproducibility, availability, standardization, or costs. This review summarizes the published literature reporting on functional imaging of vascular inflammation in atherosclerotic plaques emphasizing those techniques that have the greatest and/or most immediate potential for broad application in clinical practice. The prospective evaluation of these techniques and standardization of protocols by multinational networks could serve to determine their added value in clinical practice and guide their development and deployment.

Keywords Functional imaging • Vascular inflammation

Introduction

Atherosclerosis affects the arterial tree in a continuum. The disease may take root early in life, but it does not become clinically overt until atherosclerotic plaques reach a critical stage. Certain clinical manifestations of the disease relate to the impairment of tissue perfusion due to luminal encroachment by the growing plaque, causing impaired blood flow and symptoms such as angina pectoris. Such plaques generally have a fibrotic morphology, often referred to in shorthand as 'stable' lesions. Patients with this type of lesion have quite a low mortality rate ($\leq$3% annually). Imaging has established utility in the non-invasive diagnosis of such flow-limiting atherosclerotic lesions, informing risk stratification and allocation to an appropriate management strategy.

The development and refinement of non-invasive cardiac imaging over the past two decades has provided new tools for the identification of preclinical disease that reach beyond identification of flow-limiting stenoses. Studies using positron emission tomography (PET) for the non-invasive quantification of regional myocardial blood flow (mL/min/g) have demonstrated dysfunction of the coronary microvasculature (arterioles $<$300 μm of diameter) in asymptomatic subjects with a normal angiogram who have risk factors for CAD—such as hypercholesterolaemia, essential hypertension, diabetes mellitus, and smoking.[1,2] These studies have provided evidence of how cardiovascular risk factors alter coronary microvascular function, in the absence of stenoses of the epicardial coronary arteries. Such microvascular dysfunction without epicardial stenosis can also produce chest discomfort, a scenario that applies particularly to women.

Atherosclerosis may, however, assume another preclinical form associated with potentially devastating effects: the development of often non-obstructive, but 'unstable' arterial plaques that may rupture and provoke acute thrombosis, causing unheralded events such as acute myocardial infarction and stroke.[3,4] As anatomical imaging has matured over the last several decades, our unravelling of the cellular and molecular mechanisms of cardiovascular disease has expanded markedly. Research has identified several molecular targets, biochemical pathways, and cellular

* Corresponding author. Tel: +39 0226436202, Fax: +39 0226436218, Email: camici.paolo@hsr.it

markers that furnish expanding insight into the mechanisms of cardiovascular diseases.[5] These advances offer an enormous opportunity to expand imaging beyond the traditional anatomical and physiological domains, by harnessing these advances in basic cardiovascular biology to image particular molecular structures, cellular behaviours, and metabolic pathways, and probe the biological processes that underlie cardiovascular diseases.

Table 1 summarizes the armamentarium of non-invasive imaging techniques available for molecular imaging. Nuclear techniques, such as PET and single-photon emission computed tomography (SPECT), stand out because of their high sensitivity for small amounts of probe mass, but these modalities have relatively limited spatial resolution. In contrast, magnetic resonance imaging (MRI) and computed tomography (CT) have superior spatial resolution, but less sensitivity. Optical techniques, such as bioluminescence or fluorescence imaging, have restricted tissue penetration depth, presenting challenges to imaging deep arteries in large animals and humans. Experimental investigations have used these techniques in conjunction with a variety of molecular-targeted compounds, but few have made their way into the clinic.[6–8] While many previous reports have focused on the pathobiological features of plaque vulnerability, we shall concentrate here on those compounds and non-invasive modalities that have the greatest potential for rapid application to clinical practice.[9]

Pathobiology and targets for non-invasive imaging

Early in the formation of atherosclerotic lesions, the endothelial cells that form the interface of the arterial wall with the circulation focally change their palette of homoeostatic functions and adopt an altered molecular programme. These changes, crucial for host defences following tissue injury or infection, can prove deleterious in the context of atheroma formation. The normal arterial endothelial monolayer tonically exhibits anticoagulant, pro-fibrinolytic, vasodilator, antioxidant, and anti-inflammatory properties. When endothelial cells sense danger—as signalled by bacterial products such as endotoxin, or by molecules associated with cardiovascular risk factors such as constituents of modified low-density lipoprotein, angiotensin II, or pro-inflammatory cytokines—the homoeostatic panel of properties gives way to a predominance of pro-coagulant and anti-fibrinolytic mediators, to impairment of the vasodilator function, and often to generation of vasoconstrictor substances, as well as a gamut of pro-inflammatory functions.

Among these changes, the expression of adhesion molecules on the surface of the activated endothelial cells can capture blood leucocytes. Of these endothelial-leucocyte adhesion molecules, vascular cell adhesion molecule-1 (VCAM-1) has received considerable attention as a target for molecular imaging (*Figure 1*).[10,11] Other adhesion molecules that mediate the attachment of monocytes and T cells include the fractalkine receptor CX3CR1. In established atherosclerotic lesions, plexi of microvessels can provide a large surface area of endothelial cells that furnish an apt target for imaging (*Figure 1*). Current approaches to imaging such adhesion molecules include microbubbles linked with antibodies that recognize the adhesion molecules selectively and

Table 1 Non-invasive molecular imaging tools

Imaging modality	Form of energy used	Spatial resolution (mm)	Acquisition time per frame (s)	Molecular probe mass required (ng)	Tissue penetration depth (mm)	Mainly small animal or clinical?	Cost (equipment and usage)
PET	Annihilation photons	1–4 (animal), 4–5 (clinical)	1–300	1–100	>300	Both	High
SPECT	Gamma rays	0.5–5 (animal), 7–15 (clinical)	60–2000	1–100	>300	Both	Medium-High
Bioluminescence imaging	Visible to infrared light	3–10	10–300	10^3–10^6	1–10	Small animal	Low
Fluorescence imaging	Visible to infrared light	2–10	10–2000	10^3–10^6	1–20	Small animal	Low
MRI	Radio-frequency waves	0.025–0.1 (animal), 0.2- (clinical)	60–3000	10^3–10^6	>300	Both	High
Ultrasound	High-frequency sound waves	0.05–0.5 (animal), 0.1–1 (clinical)	0.1–100	10^3–10^6	1–200	Both	Low
CT	X-rays	0.03–0.4 (animal), 0.3–1 (clinical)	1–300	N/A	>300	Both	Medium-High

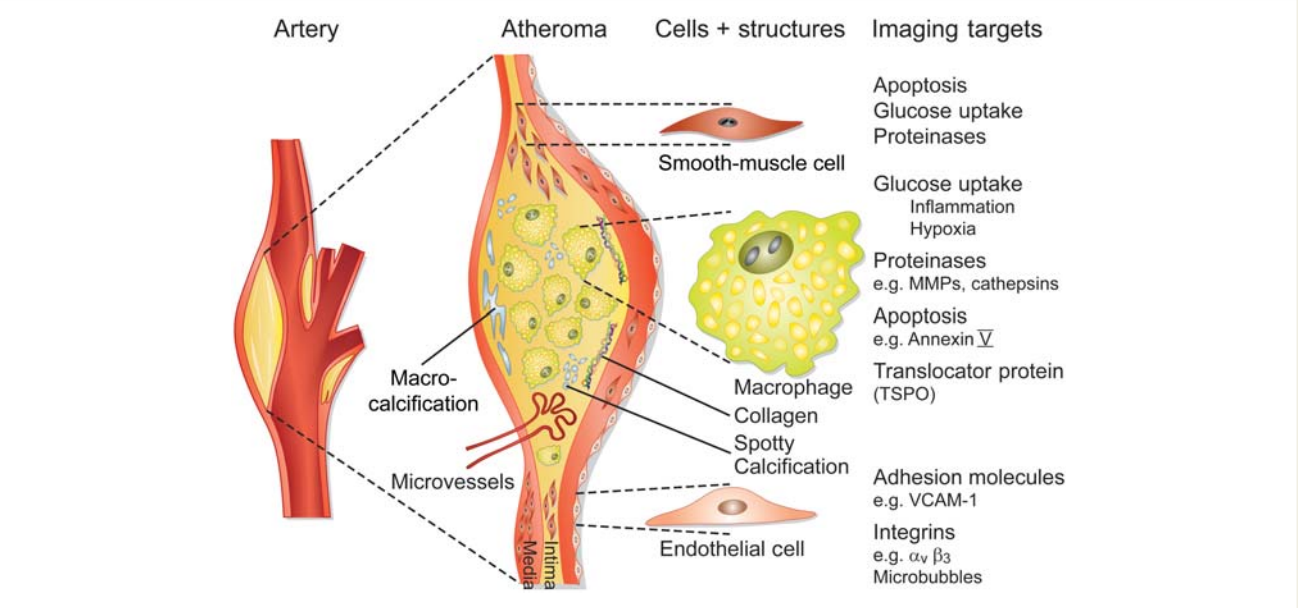

Figure 1 Imaging targets in the atherosclerotic plaque. The diagram on the left depicts a plaque in the carotid bifurcation. The exploded view in the middle illustrates the composition of the plaque (lumen to the right), showing a calcified region in blue at the base of the plaque on the left, macrophages in the lipid rich necrotic core (yellow), triple helical collagen fibrils, and smooth-muscle cells in the plaque's fibrous cap (brown) underlying the endothelial monolayer. The blue dots represent spotty calcification. The microvessels also penetrate the base of the plaque from the adventitia. Various imaging targets on the major cell types shown are listed on the right. MMPs, matrix metalloproteinases; VCAM-1, vascular cell adhesion molecule-1.

permit visualization by contrast-enhanced ultrasound (CEU). Approaches to improve the stoichiometry of the targeting moiety to the imaging moiety of an agent include the use of peptides identified by screening of phage-display libraries. Peptide-linked imaging agents that can target VCAM-1 include those coupled to near infrared fluorophores, and radionuclides.[12] The neovessels within the plaque arise by angiogenesis and often bear integrins, such as $\alpha_v\beta_3$, that have also served as targets for imaging agents.[13,14]

The most predominant leucocyte recruited to the artery wall during atherogenesis, the blood monocyte, matures into a macrophage once resident in the arterial intima (*Figure 1*). Tissue macrophages can become phagocytically active, a process very important in internalizing pathogens during host defence reactions. In the context of atherosclerosis, internalization of lipoprotein particles yields foam-cell formation. This phagocytic capacity furnishes further opportunity for imaging of a cellular process. Nanoparticles that undergo phagocytosis can provide a target for imaging of inflammatory cells. Ultra-small particulate iron oxide particles (USPIOs), rendered biocompatible with tunable kinetics in the circulatory system due to coating with dextran molecules of various chain lengths, generate an MRI signal when engulfed by plaque macrophages.[15]

Early in the response to hyperlipidaemia, lipoproteins accumulate in the intima. Sequestered from plasma antioxidants, lipids and lipoproteins that accumulate in the arterial intima undergo oxidative modification that provides another potential target for molecular imaging. Epitopes associated with oxidized phospholipids generate antibodies that, when linked to radionuclides, can report on the accumulation of modified lipoproteins in atherosclerotic lesions.[16] Lipid accumulation and the formation of modified lipids furnish other opportunities for imaging—for example, by near infrared or Raman spectroscopy.

Mononuclear phagocytes within the plaque may change their metabolic activity when undergoing inflammatory activation. As glucose uptake enjoys wide use in tumour imaging, many groups have documented increased uptake of the positron-labelled glucose analogue ^{18}F-fluorodeoxyglucose (FDG) in atheromata using PET. Thus, increased uptake of FDG may provide a marker for metabolically active inflammatory cells in plaques that could prove clinically useful, given the widespread use of this approach in oncology and availability of the tracer (see below).

Once recruited and resident in the arterial intima, mononuclear phagocytes amplify and perpetuate the local inflammatory processes by producing mediators that can contribute to the progression and complication of atherosclerotic plaques. Activated phagocytes can produce elevated levels of reactive oxygen species. Plaque macrophages can express myeloperoxidase, an enzyme that produces hypochlorous acid (HOCl), a highly pro-oxidant species. Molecular imaging techniques can visualize myeloperoxidase and its product.[17,18] Smooth-muscle cells and phagocytes within the plaque express NADPH oxidases that generate superoxide anions. Thus reporters of reactive oxygen species could provide another approach to imaging inflammation within plaques.

Considerable work has substantiated the overproduction by plaque macrophages of enzymes that catabolize constituents of the arterial extracellular matrix.[19] Breakdown of collagen and elastin, the major constituents of the arterial extracellular matrix, can prove pivotal in arterial remodelling and in weakening of the

collagenous skeleton that renders plaques susceptible to rupture and, hence, to thrombosis. In response to inflammatory mediators, virtually all cell types within atherosclerotic plaques can overexpress proteases capable of extracellular matrix degradation. The key enzymes in collagen breakdown, the interstitial collagenases, belong to the matrix metalloproteinase (MMP) family. Activated mononuclear phagocytes within plaques also overproduce elastolytic sulfhydryl proteinases such as cathepsins S, K, and L, all implicated in arterial remodelling in atherosclerosis by experimental studies. Serine proteinases, including neutrophil elastase, also may participate in arterial remodelling during atherogenesis. Several approaches can visualize such proteinases. Protease inhibitors conjugated with radionuclides constitute one approach to visualizing MMPs. Proteolytic cleavage of quenched fluorescence substrates makes use of the catalytic potential of these enzymes. While inhibitors bind in a one-to-one stoichiometry to the proteases, a single enzyme molecule can cleave many substrate molecules using catalysis to amplify the fluorescent signal. Although animal experiments have validated the utility of both approaches, extension to humans requires further work.[20–22] Notably, the development of intra-vascular probes that can detect near infrared fluorescent signals can provide a platform for translation of these optical approaches to humans, albeit invasively.[23]

Advanced human atherosclerotic plaques contain zones of fibrosis. Accumulation of gadolinium, detectable by MRI, may allow visualization of plaque fibrosis, vascularity, or permeability using existing imaging agents and platforms.[24,25] Calcification within atherosclerotic plaques reflects a dynamic biological process, not mere mineral accretion, and gives a strong signal on CT. Thus, visualization of calcification, including regions of spotty calcification that can promote plaque instability, provides another window on a biological feature of plaques that may reflect inflammatory activation (*Figure 1*).[26] Although fibrosis and calcification may be targets for molecular imaging, they may characterize 'stable' lesions as well as those prone to rupture and thrombosis.

Ultimately, mononuclear phagocytes within plaques can die either by oncosis or by programmed cell death (apoptosis). Cells undergoing apoptosis characteristically exteriorize phosphatidyl serine. The protein annexin V, bound to radionuclides, can visualize apoptotic cells. As apoptosis may occur more frequently in lipid-rich plaques with ongoing inflammation, markers of this biological process may also provide a probe into aspects of plaque biology that relate to their complication.[27] Thus, from the nascent atherosclerotic plaque to the death of inflammatory and vascular cells, molecular imaging approaches provide an exciting new window on visualizing biological processes that may contribute to plaque evolution, and ultimately to thrombotic complication.

Positron emission tomography

The serendipitous observation that some arteries can take up FDG administered for tumour visualization has spawned much interest in using this convenient and well-established agent to visualize atherosclerosis.[28] The first clinical study of PET-FDG imaging of human atherosclerosis was published in 2002, and it demonstrated increased FDG uptake in carotid plaques associated with recent cerebrovascular ischaemic events.[29] When tissue from human atherosclerotic plaques, obtained following endarterectomy, was incubated *ex vivo* with tritiated deoxyglucose, the tracer was taken up by plaque macrophages, but not by surrounding vascular smooth-muscle cells or by normal vessels. Subsequent studies have shown that the uptake of FDG correlates significantly with plaque macrophage content, and is ~20 times higher in the most inflamed plaques than in control arteries.[30,31] The use of PET-FDG imaging has been extended to other large arteries of the body (aorta, femoral, and iliac arteries) since then.[28,32] The FDG signal in atherosclerotic plaques correlates well with circulating inflammatory biomarkers,[28,33] older age,[34] male sex,[35] and the presence of traditional cardiovascular risk factors.[33,36] Additionally, some studies have documented a good short-term inter-scan repeatability (2 weeks to 3 months), an important prerequisite for studies using FDG uptake as a surrogate endpoint for plaque-stabilizing treatments.[28,37] Early pilot studies using a high-fat dietary preparation to prevent spillover artefacts from myocardial FDG uptake have also demonstrated that coronary and aortic FDG uptake often associates with symptoms of acute myocardial ischaemia.[38,39]

These observations led to the conclusion that the FDG signal in atheromata reports on inflammation. Several groups have shown that interventions—notably, treatment with HMG-CoA reductase inhibitors (statins)—can reduce FDG signals.[40,41] Effective therapeutic intervention to reduce FDG uptake has raised hope that FDG signals can allow evaluation of novel therapeutics that may alter inflammation in atherosclerotic plaques. Indeed, several dozen clinical trials currently underway use FDG uptake as a biomarker of inflammation within plaques.

Despite these attractions, some issues require resolution before embracing FDG uptake in this regard. Firstly, only limited prospective data correlate FDG uptake, or changes in FDG uptake, with cardiovascular events or altered rates of such complications,[42] and we eagerly await the results of larger prospective cohort studies, such as the High Risk Plaque Initiative and BioImage studies.[43,44] We lack sufficient validation of the ability of multicentre studies to provide standardized data on FDG uptake. Information regarding false positives, false negatives, sensitivity, and reproducibility on longitudinal follow-up remains rudimentary. Although FDG signals that co-localize with carotid atheromata present little difficulty with identifying the region of interest, and show modest background signal, considerable barriers to using FDG uptake to visualize coronary atheromata exist—because of avid glucose uptake by myocytes, and substantial myocardial background even under conditions of high-dietary fat intake to suppress cardiac myocyte FDG uptake.

In addition, mechanisms other than inflammation may generate FDG signal associated with atheromata. Microvessels in the plaque may increase delivery of the radiolabelled glucose analogue, enriching its local-specific radioactivity in the glucose pool and giving rise to greater accumulation within cells and signal generation that may not reflect absolute increases in glucose transport. Other biological processes, including hypoxia, may drive increased glucose utilization by mononuclear phagocytes, a putative major source of the FDG signal in atheromata.[45] In particular, studies of human mononuclear phagocytes have not consistently shown increased glucose uptake in response to pro-inflammatory mediators. In contrast, hypoxia readily stimulates glucose uptake by these

cells. Hence hypoxia, rather than inflammation, may increase glucose and hence FDG uptake by inflammatory cells in atheromata. In addition, statins can decrease hypoxia-induced augmentation in glucose uptake in human mononuclear phagocytes *in vitro*.[45] Thus, the attenuation of the FDG signal by statins may not necessarily reflect an anti-inflammatory action. In this regard, nuclear agents that image hypoxia, already in use in oncology, may be useful in imaging atherosclerosis, as hypoxic conditions may prevail in the core of lesions.[45]

Moreover, some have questioned the specificity of FDG for activated macrophages. A micro-autoradiography study of aortic sections of ApoE$^{-/-}$ mice showed a poor correlation of ^{14}C-FDG uptake with fat content and selective macrophage staining with anti-CD68 in atherosclerotic plaques.[46] Davies *et al.*[47] reported that, at variance with *ex vivo* findings, *in vivo* FDG micro-PET uptake in atherosclerotic lesions of rabbit aorta did not correlate with macrophage accumulation ($r = 0.16$, $P = 0.57$), and that FDG uptake in rabbits with highly inflamed aortic walls, those with low levels of inflammation, or controls did not differ significantly. In summary, although FDG has many attractive aspects for clinical use in characterizing atheromata, its underlying biological mechanisms and clinical significance remain incompletely understood and validated. As a result, other compounds have emerged for interrogating vascular inflammation with PET.

The ^{11}C-labelled PET tracer PK11195 is a selective ligand of the translocator protein (TSPO, 18 kDa), formerly known as peripheral benzodiazepine receptor.[48] Translocator proteins were discovered in the 1970s as benzodiazepine-binding sites outside the central nervous system.[49] Subsequent studies have shown a high TSPO density in circulating human phagocyte populations, particularly in monocytes and neutrophils, with up to 750 000 binding sites per cell.[50] Mature monocytic cell lines have higher TSPO expression than do pro-monocytic or pro-myelocytic lines. Levels of TSPO increase two- to three-fold after monocyte activation *in vitro* with interferon-gamma or phorbol 12-myristate 13-acetate. Stimulated human monocytes can express >2 000 000 binding sites for PK11195. This increase accompanies enhanced expression of CD11a and CD11b surface antigens and increased production of interleukin-1, interleukin-8, and tumour necrosis factor, indicating that TSPO over-expression associates with activation of phagocytes.[51] ^{11}C-PK11195 has been used extensively for the non-invasive imaging of neuroinflammatory and neurodegenerative conditions due to its high uptake in activated microglia and low uptake in neurons.[52] Subsequent studies have demonstrated uptake of ^{11}C-PK11195 by synovial macrophages in patients with rheumatoid arthritis.[53]

Fujimura *et al.*[54] showed specific binding of ^{3}H-PK11195 to macrophages in samples of human carotid atherosclerotic plaque. In a small proof-of-concept study by Pugliese *et al.*[55] in patients with large-vessel vasculitis (predominantly giant-cell arteritis and Takayasu arteritis), ^{11}C-PK11195 PET/CT allowed detection and quantification of aortic inflammation. Of 15 patients, all 6 patients with signs and symptoms of active vasculitis (visual disturbance, headache, bruit or vascular pain/tenderness, new claudication, fever, night sweats, and/or arthralgia) had markedly increased vascular uptake of ^{11}C-PK11195 [target-to-background ratio (TBR), 2.41], whereas patients with quiescent disease had background uptake (TBR, 0.98). Standardized uptake values for ^{11}C-PK11195 correlated well with quantitative total intra-plaque volumes of distribution, calculated from dynamic tissue kinetic modelling using a 1-tissue compartment model.[56] In a subsequent study from the same group, 32 patients with carotid stenoses (of which 9 had recently suffered an acute cerebrovascular ischaemic event) underwent ^{11}C-PK11195 PET/CT angiographic (CTA) imaging.[57] Carotid plaques associated with ipsilateral symptoms [stroke or transient ischaemic attack (TIA)] had higher TBR (1.06 ± 0.20 vs. 0.86 ± 0.11, $P = 0.001$) and lower CT attenuation [(median, interquartile range) 37, 24–40 vs. 71, 56–125 Hounsfield units, $P = 0.01$] than those without ipsilateral symptoms (*Figure 2*). Eight patients underwent carotid endarterectomy, and plaques were harvested for *ex vivo* analysis: on immunohistochemistry and confocal fluorescence microscopy, CD68 and TSPO co-localized with ^{3}H-PK11195 uptake at autoradiography. ^{11}C-PK11195 TBR correlated significantly with percentage specific binding of ^{3}H-PK11195 determined by autoradiography ($r = 0.77$, $P = 0.025$).

These preliminary results indicate that ligands of the TSPO hold promise as molecular-targeted imaging compounds to interrogate the presence of intra-plaque inflammation in patients with atherosclerotic disease, and should encourage further prospective studies to assess the predictive value of ^{11}C-PK11195 or similar TSPO ligands for cardiovascular events. Extending ^{11}C-PK11195 PET/CT imaging to the coronary arteries represents a great challenge due to the small vessel calibre, the relatively low spatial resolution of PET, and cardiac and respiratory motion. Nonetheless, a preliminary report of imaging temporal arteritis with ^{11}C-PK11195 PET/CT demonstrates its feasibility in smaller arteries (with a diameter of ~2 mm).[58] Moreover, myocardial uptake of ^{11}C-PK11195 should be lower than for FDG, thus causing less confounding effects from background signal for imaging coronary arteries. The short physical half-life (20 min) of ^{11}C-PK11195, which mandates an on-site cyclotron facility, may limit wide clinical applicability. But newly introduced ^{18}F-labelled TSPO ligands, currently undergoing preclinical investigation, have shown applicability across species in the brain and may overcome some of these barriers.[59]

Computed tomography

Traditionally, CT angiography is an anatomical imaging modality with limited functional imaging capabilities. Its high temporal and spatial resolution allow detailed anatomical delineation of large- and medium-sized vessels and have advanced CT angiography as the most accurate and robust clinical method for non-invasive coronary angiography. Additionally, co-registration of CT angiograms with functional techniques such as PET, SPECT, or MRI (in a hybrid approach) allows the allocation of focal functional signals to micro-anatomical structures. The high CT attenuation of calcified structures allows a simple qualitative characterization of plaque composition by dividing coronary lesions into calcified, non-calcified, and mixed plaques (*Figure 3*).[60] With regard to non-calcified plaques, however, we lack persuasive evidence suggesting reliable sub-classification of plaques as lipid-rich vs. fibrous, based on CT density measurements. Different studies report wide overlap in Hounsfield units for lipid-rich vs. fibrous plaques. Reasons for this overlap include the relatively limited spatial

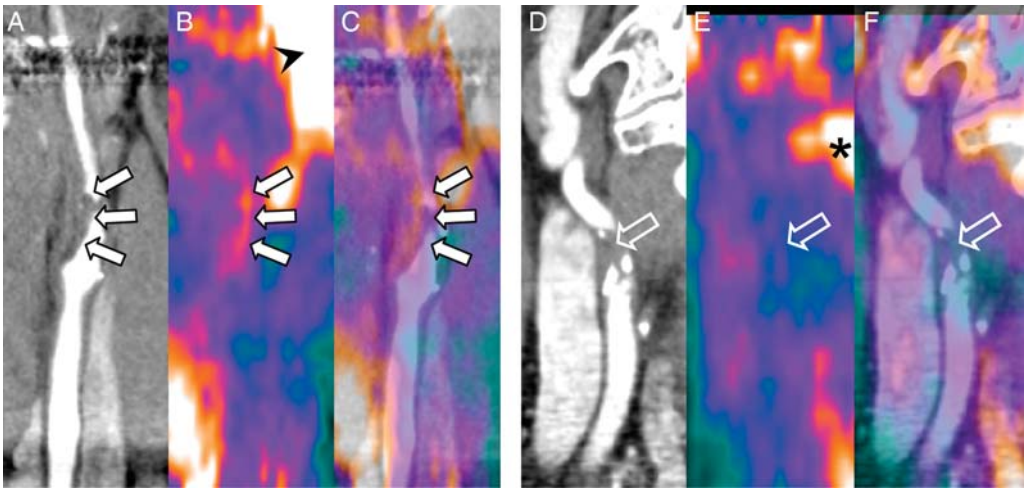

Figure 2 Computed tomography angiography (*A*), [^{11}C]-PK11195 positron emission tomography (*B*), and positron emission tomography/computed tomography fusion (*C*) in a 66-year-old right-handed male patient with a 90% left internal carotid artery stenosis (*solid arrows*) who developed a facial droop and dysphasia 3 weeks before the positron emission tomography study. Note focal [^{11}C]-PK11195 uptake along the convexity of the plaque (*B*, *C*, solid arrows). In contrast, images in a 78-year-old asymptomatic female patient with an 80% right ICA stenosis (*D*–*F*). There is no visible [^{11}C]-PK11195 uptake in the region of the plaque (*open arrows*). The black arrowhead denotes high [^{11}C]-PK11195 uptake in the submandibular gland, and the asterisk denotes high uptake in bone marrow. Reproduced with permission from Pugliese *et al.*[55]

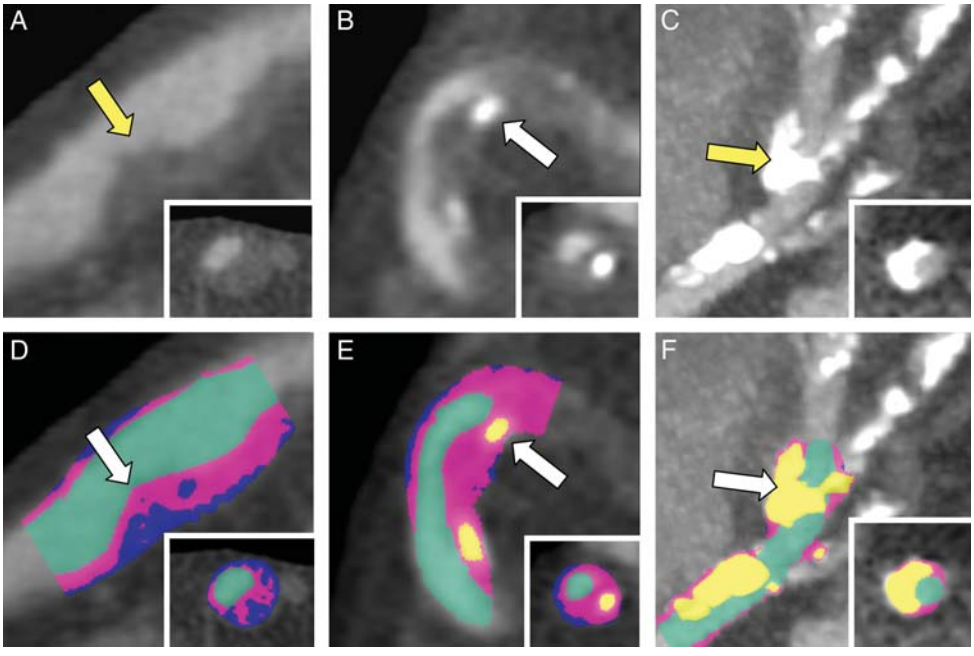

Figure 3 Qualitative characterization of coronary plaques as non-calcified (*A*), mixed (*B*), and calcified (*C*) by computed tomography angiography. Pixelwise characterization of plaque composition based on CT tissue density (Hounsfield units, HU) (*D*–*F*). Blue denotes soft tissue components with low density (<30 HU, presumably lipid-rich necrotic tissue), pink denotes soft-tissue components with high density (>30 HU, presumably fibrous tissue), and yellow denotes calcified components (>460 HU). The green area indicates contrast-filled coronary lumen. The insets show representative cross sections of the coronary artery taken at the site of the arrow. Courtesy of Philipp A. Kaufmann, Cardiac Imaging, University Hospital Zurich.

resolution of CTA (with subsequent partial volume effects) and a variable intra-plaque contrast uptake interfering with the native density of plaque components.[61] Finally, CTA cannot yet identify plaques with thin fibrous caps [so-called thin-cap fibro-atheroma (TCFA)], as current devices lack the spatial resolution to detect the thickness of the fibrous cap (~65 μm), although some TCFA may produce a ring-like enhancement on CTA.[62]

Several other plaque characteristics on CTA associate with acute ischaemic events. A few small retrospective studies have consistently shown that culprit lesions of acute coronary syndromes (ACS) had larger vessel areas, more positive remodelling, and a higher proportion of non-calcified and mixed plaque components.[63] Hoffmann *et al.*[64] demonstrated a significantly larger plaque area (17.5 vs. 13.5 mm^2) and a higher remodelling index (1.4 vs. 1.2) in culprit lesions of ACS patients, compared with patients with stable angina. One retrospective study in 71 patients showed that culprit lesions in patients with ACS had more positive remodelling (87 vs. 12%), more low-density (<30 Hounsfield units) plaque components (79 vs. 9%), and a higher prevalence of 'spotty' calcifications (63 vs. 21%).[65] A prospective validation study confirmed the former two features as significant predictors of ACS in >1000 patients.[66] Pundziute *et al.*[60] observed a higher prevalence of non-calcified and mixed plaques among culprit lesions of ACS patients (32 and 59%, respectively), while stable angina patients more commonly had calcified lesions (61%). IVUS-defined TCFAs in ACS patients associated most frequently with lesions classified as mixed on CTA.

Finally, CT has shown promising preliminary results in the context of molecular imaging of intra-plaque inflammation using targeted nanoparticle contrast agents. The compound N1177 is a suspension composed of crystalline iodinated particles dispersed with surfactant with a high affinity to activated macrophages.[67] In atherosclerotic rabbits, CT density of plaques after N1177 injection correlated with FDG uptake.[68] But despite encouraging findings in animals, some have raised concerns about the low sensitivity of CT to detect molecular contrast agents.[69] Spectral (or multicolour) CT, which can identify types of tissue based on their characteristic energy-dependent photon attenuation, may thereby enhance the sensitivity of CT to detect targeted contrast agents. In atherosclerotic mice, spectral CT enabled detection of intra-plaque inflammation after injection of gold-labelled high-density lipoprotein nanoparticles designed to target activated macrophages.[70] The feasibility and clinical applicability of CT for molecular imaging of plaque vulnerability awaits clinical translation to humans.

Magnetic resonance imaging

The combination of multiple MR sequences, either with bright-blood [time-of-flight (TOF)] or black-blood flow suppression,[71,72] can identify the main components of vascular lesions (*Figure 1*)—such as the fibrous cap,[73] lipid-rich necrotic core (LRNC),[74–76] intra-plaque haemorrhage,[77–79] neovasculature,[80,81] and signs of vascular wall inflammation.[82–85]

Emerging evidence links biomechanical forces to the pathogenesis of plaque vulnerability,[86–89] and to the timing of symptoms.[90] Using MRI and finite element analysis to calculate the mechanical stress within carotid plaques, Sadat *et al.*[90] suggested that the maximum circumferential stress within the plaques of patients with acute symptoms exceeds that in plaques of recently symptomatic patients, and that plaques associated with recurrent TIAs had significantly higher stress than those associated with a single episode of TIA.[91]

Extensive MRI studies have validated the characterization of vulnerable plaques, including LRNC and the thin fibrous cap, by histological analysis of retrieved endarterectomy specimens.[77,92] At 1.5 T, bright-blood TOF images show the intact fibrous cap as a continuous hypo-intense band against the bright lumen with a smooth surface. Discontinuity of the hypo-intense band, juxtaluminal hyperintensity in TOF and T1-weighted images (indicating recent haemorrhage), and an irregular surface characterize fibrous cap rupture. Mitsumori *et al.*[73] reported 81% sensitivity and 90% specificity at 1.5 T for identifying a thin, ruptured fibrous cap. The LRNC has a high content of cholesterol and cholesteryl esters that have short transverse relaxation (T2), resulting in a hypo-intense signal in T2-weighted images. Using multi-sequence (T1-weighted, T2-weighted, proton density, and 3D TOF) imaging, Yuan *et al.*[77] found high sensitivity (85%) and specificity (92%) for the identification of LRNC.

Fibrous cap rupture detected by MRI associates with symptoms[93] or cerebrovascular accidents.[94] Interestingly, in patients with mild-to-moderate stenosis, the thin/ruptured fibrous cap associated significantly with LRNC and symptoms, whereas in patients with severe stenosis, only the presence of ulceration at MR angiography associated with symptoms.[93] In 138 asymptomatic patients who had a 50–79% carotid stenosis, those patients whose plaques were characterized by thinned or ruptured fibrous caps, large LRNC, intra-plaque haemorrhage (IPH), and large maximum wall thickness had a higher incidence of cerebrovascular accidents.[95] As stated earlier, activation of mononuclear phagocytes promotes the evolution of the atherosclerotic lesion. Two MRI strategies may delineate macrophage accumulation in the atheromatous plaque: (i) dynamic kinetics of tissue enhancement after administration of gadolinium contrast; (ii) USPIOs that target macrophages *in vivo*. Enhancement of plaque tissue with gadolinium contrast may link directly to increased highly permeable vascular supply within the plaque. The transfer constant (K^{trans}) of gadolinium into the extravascular extracellular space, calculated from dynamic kinetics of tissue enhancement, correlates strongly with macrophage content, and to a lesser extent with neovasculature and loose matrix areas measured at histology.[96] Interestingly, K^{trans} associates significantly with low HDL levels and smoking, but not with recent cerebral ischaemic symptoms.

As noted above, activated macrophages infiltrating the plaque engulf USPIOs rendered biocompatible by coating with materials such as dextran.[84,97] The internalization of the ferromagnetic USPIOs leads to a change in the resonance frequency of surrounding water molecules and a shortening of their relaxation times, which appears as a signal loss in T2-weighted sequences (*Figure 4*). In human plaques, however, the loss of signal also reflects other features such as a partial volume effect, local haemorrhage, and calcification. Several techniques to generate a positive signal with high signal-to-noise ratio are under investigation.[98,99] USPIOs may have slow uptake, requiring long circulating times to

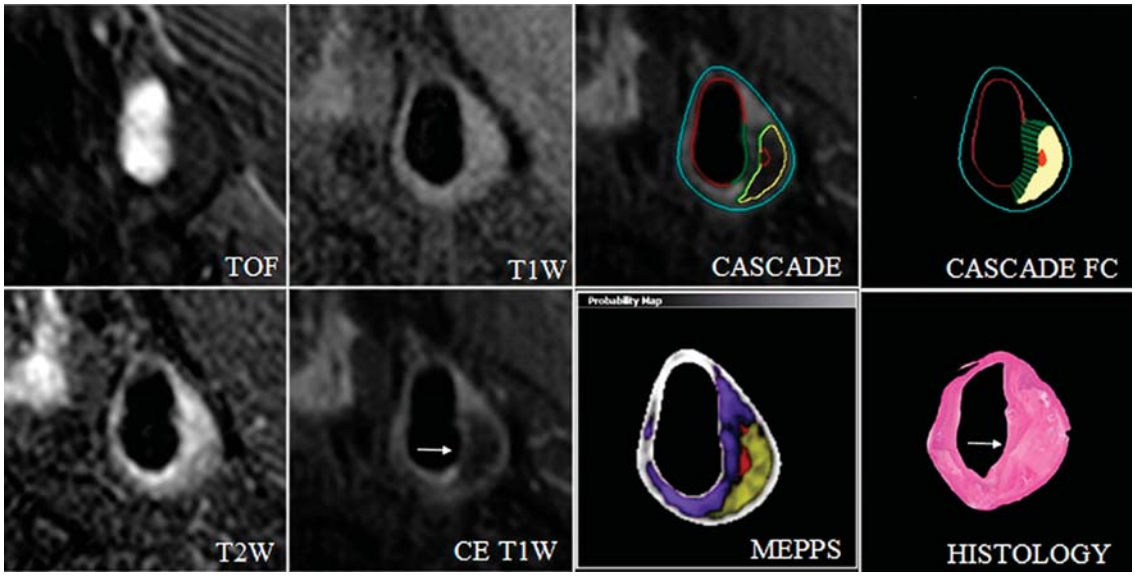

Figure 4 Automated segmentation of bright- and black-blood, high-spatial-resolution, multi-contrast *in vivo* magnetic resonance imaging. Quantification of *in vivo* magnetic resonance imaging (TOF, T1W, T2W, and CE T1W) using CASCADE to generate component outlines. The CASCADE fibrous cap is an additional algorithm that collects the fibrous cap length, depth, and area. The automated map of the plaque is produced by the MEPPS algorithm. The loose matrix is shown in *purple*, lipid-rich necrotic core in *yellow*, and intra-plaque haemorrhage in *red* on the MEPPS image. Histology from a carotid endarterectomy sample confirms the components and the enhancing thick fibrous cap (*arrow*). *In vivo* CMR were acquired on a 3T scanner along with the use of an eight-element phased-array carotid coil. CASCADE, computer-aided system for cardiovascular disease evaluation; CE, contrast-enhanced; CEA, carotid endarterectomy; MEPPS, morphology-enhanced probabilistic plaque segmentation; TOF, time-of-flight; T1W, T1-weighted; T2W, T2-weighted. Reproduced with permission from Chu B, Ferguson MS, Chen H, *et al.* Magnetic resonance imaging features of the disruption-prone and the disrupted carotid plaque J Am Coll Cardiol Img 2009; 2:883–896.

obtain an adequate accumulation allowing a good signal-to-noise ratio.[100] Notwithstanding these practical and theoretical limitations, the ATHEROMA trial used USPIOs in 40 patients to demonstrate that aggressive lipid-lowering therapy with atorvastatin over a 3-month period associated with a significant reduction in plaque uptake.[101]

Intra-plaque haemorrhage can originate from rupture of the vasa vasorum,[102] and localize deep in the core of the lesion or occur from fissures at the luminal surface.[103] The degradation of haemoglobin to methaemoglobin shortens the relaxation (T1) time. As a consequence, recent haemorrhage appears as a bright signal on black-blood T1-weighted sequences and magnetization-prepared rapid acquisition gradient echo (MP-RAGE).[104] A few MRI studies have suggested a role for IPH in plaque destabilization, and its association with subsequent cerebrovascular events.[78,105,106] More recently, Zhao *et al.*[107] questioned this role in a study of 181 patients with carotid stenoses >50%. The use of MR coronary angiography remains predominantly investigational, and the characterization of coronary artery plaques adds to the technical challenges. Using T1-weighted black-blood inversion recovery before (N-IR) and after administration of gadolinium contrast (CE-IR), Maintz *et al.*[108] made an effort to classify the coronary plaques of CAD patients as hypo-intense on N-IR and CE-IR (type 1), hyperintense both on N-IR and on CE-IR (type 2), and hypo-intense on N-IR and hyperintense on CE-IR (type 3). Contrast uptake may link to both inflammation and fibrosis; however, the correlation of these features with the progress of disease remains poorly understood, and awaits confirmation in larger-scale studies.

Contrast-enhanced ultrasonography

Targeted microbubbles have undergone experimental evaluation for visualizing cell surface structures implicated in plaque rupture.[109,110] The compressible gas bubbles produce acoustic energy by resonating or releasing free gas when insonated. Most studies involving microbubble-based imaging agents have used antibodies as the targeting moiety. Other targeting strategies have involved the use of peptides and glycoproteins. Targets successfully visualized experimentally with contrast-induced ultrasound include leucocyte adhesion molecules such as intracellular adhesion molecule-1, VCAM-1, and P-selectin (*Figure 1*). Antibodies that recognize glycoprotein IIb/IIIa or peptides that contain the RGD sequence have succeeded experimentally in imaging activated platelets in thrombi. Targeting integrins such as $\alpha_v\beta_3$ also may serve to visualize microvessels. Unlabelled microbubbles can delineate neovascular channels in atherosclerotic plaques or the surrounding adventitia, providing another window on the characteristics associated with plaques at high risk of rupture.[111,112]

Limitations of contrast-enhanced ultrasound include the short half-life of these bubbles *in vivo*, their restriction to the intravascular compartment, and the low contrast-to-noise ratio. Advantages include the very large installed base of ultrasound apparatuses, and the familiarity of this modality to practicing clinicians. Moreover, the lack of ionizing radiation also renders this approach attractive for routine clinical use.

Conclusions

Findings from the clinic and the laboratory during the last several decades have revolutionized our thinking about the mechanisms of thrombotic complications of atherosclerosis. The traditional focus on stenosis has given way to the recognition that microanatomical and biological aspects of plaques also influence the propensity to provoke thrombotic complications. Advances in anatomical imaging open up the prospect of non-invasive approaches to defining the features of atheromata associated with clinical complications. Progress in the understanding of the biological basis of plaque disruption has identified molecular and cellular targets that extend the scope of imaging beyond anatomy. The field of imaging of atherosclerosis seems poised at the threshold of exciting new advances.

Yet, we still need to confront several substantive challenges to make clinical imaging of the rupture-prone plaque a reality. Each modality discussed here faces limitations with respect to widespread application to patients, particularly with the goal of identifying plaques with characteristics of instability in the coronary circulation. Production of some molecular probes requires access to a cyclotron and radiopharmacy facilities capable of good manufacturing practices (GMP)-level production. While often available in specialized centres, the installed base of the infrastructure for advanced imaging may limit dissemination of its routine use in patients. Moreover, myocardial background uptake has presented particular challenges for coronary arterial imaging with FDG. Radiation exposure and the difficulty of molecular targeting with radio-iodinated contrast agents present barriers to the clinical application of computed tomographic techniques to identify so-called vulnerable plaques. On the other hand, while well-validated sequences and dedicated coils are available for obtaining images of the carotid arteries and 'vulnerable' plaques with MRI, cardiac and respiratory motion restricts the current effectiveness of MRI in the coronary tree. New techniques that have proved promising in animal experiments—including near-infrared detection of fluorescent probes and contrast-enhanced ultrasound—likewise have limits with respect to platforms for non-invasive detection of optical signals, and contrast-to-noise ratios in the ultrasound arena.

As more groups focus on novel approaches to imaging atherosclerosis worldwide, and with appropriate academic–industrial partnerships and public funding, many of these barriers should prove superable. Technology-intensive imaging modalities will likely not prove cost-effective in widespread screening, and will require careful consideration of indications for routine clinical use. Nonetheless, practical approaches to the imaging of inflammation and plaque at high risk of rupture will teach us a great deal about the human biology of atherosclerotic complications. The advent of such tools could prove immensely helpful in the development and testing of novel therapeutics for atherosclerotic disease, and could help us confront the unmet medical need of the residual burden of atherosclerotic events in the face of a growing global epidemic. Meanwhile, small, prospective, proof-of-principle studies to evaluate the ability of these new techniques to predict events in patients at risk of plaque rupture could provide indispensable information on their clinical value, and guide future developments.

Acknowledgements

The authors wish to acknowledge the invaluable help of Ms Sara Karwacki in the preparation of the manuscript.

Conflict of interest: O.G., P.L., and O.E.R. have no conflicts to disclose. P.G.C. has worked as a consultant for General Electric Health Care and Servier International.

References

1. Camici PG, Crea F. Coronary microvascular dysfunction. *N Engl J Med* 2007;**356**:830–840.
2. Recio-Mayoral A, Mason JC, Kaski JC, Rubens MB, Harari OA, Camici PG. Chronic inflammation and coronary microvascular dysfunction in patients without risk factors for coronary artery disease. *Eur Heart J* 2009;**30**:1837–1843.
3. Naghavi M, Libby P, Falk E, Casscells SW, Litovsky S, Rumberger J, Badimon JJ, Stefanadis C, Moreno P, Pasterkamp G, Fayad Z, Stone PH, Waxman S, Raggi P, Madjid M, Zarrabi A, Burke A, Yuan C, Fitzgerald PJ, Siscovick DS, de Korte CL, Aikawa M, Juhani Airaksinen KE, Assmann G, Becker CR, Chesebro JH, Farb A, Galis ZS, Jackson C, Jang IK, Koenig W, Lodder RA, March K, Demirovic J, Navab M, Priori SG, Rekhter MD, Bahr R, Grundy SM, Mehran R, Colombo A, Boerwinkle E, Ballantyne C, Insull W Jr, Schwartz RS, Vogel R, Serruys PW, Hansson GK, Faxon DP, Kaul S, Drexler H, Greenland P, Muller JE, Virmani R, Ridker PM, Zipes DP, Shah PK, Willerson JT. From vulnerable plaque to vulnerable patient: a call for new definitions and risk assessment strategies: Part I. *Circulation* 2003;**108**:1664–1672.
4. Virmani R, Burke AP, Farb A, Kolodgie FD. Pathology of the vulnerable plaque. *J Am Coll Cardiol* 2006;**47**(8 Suppl):C13–C18.
5. Sanz J, Fayad ZA. Imaging of atherosclerotic cardiovascular disease. *Nature* 2008;**451**:953–957.
6. Langer HF, Haubner R, Pichler BJ, Gawaz M. Radionuclide imaging: a molecular key to the atherosclerotic plaque. *J Am Coll Cardiol* 2008;**52**:1–12.
7. Rudd JHF, Hyafil F, Fayad ZA. Inflammation imaging in atherosclerosis. *Arterioscler Thromb Vasc Biol* 2009;**29**:1009–1016.
8. Sinusas AJ, Bengel F, Nahrendorf M, Epstein FH, Wu JC, Villanueva FS, Fayad ZA, Gropler RJ. Multimodality cardiovascular molecular imaging, part I. *Circ Cardiovasc Imaging* 2008;**1**:244–256.
9. Buxton DB, Antman M, Danthi N, Dilsizian V, Fayad ZA, Garcia MJ, Jaff MR, Klimas M, Libby P, Nahrendorf M, Sinusas AJ, Wickline SA, Wu JC, Bonow RO, Weissleder R. Report of the National Heart, Lung, and Blood Institute Working Group on the translation of cardiovascular molecular imaging. *Circulation* 2011;**123**:2157–2163.
10. Nahrendorf M, Jaffer FA, Kelly KA, Sosnovik DE, Aikawa E, Libby P, Weissleder R. Noninvasive vascular cell adhesion molecule-1 imaging identifies inflammatory activation of cells in atherosclerosis. *Circulation* 2006;**114**:1504–1511.
11. Kaufmann BA, Sanders JM, Davis C, Xie A, Aldred P, Sarembock IJ, Lindner JR. Molecular imaging of inflammation in atherosclerosis with targeted ultrasound detection of vascular cell adhesion molecule-1. *Circulation* 2007;**116**:276–284.
12. Nahrendorf M, Keliher E, Panizzi P, Zhang H, Hembrador S, Figueiredo J-L, Aikawa E, Kelly K, Libby P, Weissleder R. ^{18}F-4V for PET-CT imaging of VCAM-1 expression in inflammatory atherosclerosis. *J Am Coll Cardiol Img* 2009;**2**:1213–1222.
13. Winter PM, Morawski AM, Caruthers SD, Fuhrhop RW, Zhang H, Williams TA, Allen JS, Lacy EK, Robertson JD, Lanza GM, Wickline SA. Molecular imaging of angiogenesis in early-stage atherosclerosis with alpha(v)beta3-integrin-targeted nanoparticles. *Circulation* 2003;**108**:2270–2274.
14. Ellegala DB, Leong-Poi H, Carpenter JE, Klibanov AL, Kaul S, Shaffrey ME, Sklenar J, Lindner JR. Imaging tumor angiogenesis with contrast ultrasound and microbubbles targeted to alpha(v)beta3. *Circulation* 2003;**108**:336–341.

15. Morishige K, Kacher DF, Libby P, Josephson L, Ganz P, Weissleder R, Aikawa M. High-resolution MRI enhanced with superparamagnetic nanoparticles measures macrophage burden in atherosclerosis. *Circulation* 2010;**122**:1707–1715.
16. Briley-Saebo KC, Shaw PX, Mulder WJ, Choi SH, Vucic E, Aguinaldo JG, Witztum JL, Fuster V, Tsimikas S, Fayad ZA. Targeted molecular probes for imaging atherosclerotic lesions with magnetic resonance using antibodies that recognize oxidation-specific epitopes. *Circulation* 2008;**117**:3206–3215.
17. Shepherd J, Hilderbrand SA, Waterman P, Heinecke JW, Weissleder R, Libby P. A fluorescent probe for the detection of myeloperoxidase activity in atherosclerosis-associated macrophages. *Chem Biol* 2007;**14**:1221–1231.
18. Nahrendorf M, Sosnovik D, Chen JW, Panizzi P, Figueiredo JL, Aikawa E, Libby P, Swirski FK, Weissleder R. Activatable magnetic resonance imaging agent reports myeloperoxidase activity in healing infarcts and noninvasively detects the antiinflammatory effects of atorvastatin on ischemia-reperfusion injury. *Circulation* 2008;**117**:1153–1160.
19. Dollery CM, Libby P. Atherosclerosis and proteinase activation. *Cardiovasc Res* 2006;**69**:625–635.
20. Quillard T, Tesmenitsky Y, Croce K, Travers R, Shvartz E, Koskinas KC, Sukhova G, Aikawa E, Aikawa M, Libby P. Selective inhibition of matrix metalloproteinase 13 (MMP-13) increases collagen content of established mouse atheromata. *Arterioscler Thromb Vasc Biol* 2011;**31**:2464–2472.
21. Razavian M, Tavakoli S, Zhang J, Nie L, Dobrucki LW, Sinusas AJ, Azure M, Robinson S, Sadeghi MM. Atherosclerosis plaque heterogeneity and response to therapy detected by *in vivo* molecular imaging of matrix metalloproteinase activation. *J Nucl Med* 2011;**52**:1795–1802.
22. Fujimoto S, Hartung D, Ohshima S, Edwards DS, Zhou J, Yalamanchili P, Azure M, Fujimoto A, Isobe S, Matsumoto Y, Boersma H, Wong N, Yamazaki J, Narula N, Petrov A, Narula J. Molecular imaging of matrix metalloproteinase in atherosclerotic lesions: resolution with dietary modification and statin therapy. *J Am Coll Cardiol* 2008;**52**:1847–1857.
23. Jaffer FA, Calfon MA, Rosenthal A, Mallas G, Razansky RN, Mauskapf A, Weissleder R, Libby P, Ntziachristos V. Two-dimensional intravascular near-infrared fluorescence molecular imaging of inflammation in atherosclerosis and stent-induced vascular injury. *J Am Coll Cardiol* 2011;**57**:2516–2526.
24. Larose E, Kinlay S, Selwyn AP, Yeghiazarians Y, Yucel EK, Kacher DF, Libby P, Ganz P. Improved characterization of atherosclerotic plaques by gadolinium contrast during intravascular magnetic resonance imaging of human arteries. *Atherosclerosis* 2008;**196**:919–925.
25. Dong L, Kerwin WS, Chen H, Chu B, Underhill HR, Neradilek MB, Hatsukami TS, Yuan C, Zhao XQ. Carotid artery atherosclerosis: effect of intensive lipid therapy on the vasa vasorum–evaluation by using dynamic contrast-enhanced MR imaging. *Radiology* 2011;**260**:224–231.
26. Aikawa E, Nahrendorf M, Figueiredo JL, Swirski FK, Shtatland T, Kohler RH, Jaffer FA, Aikawa M, Weissleder R. Osteogenesis associates with inflammation in early-stage atherosclerosis evaluated by molecular imaging *in vivo*. *Circulation* 2007;**116**:2841–2850.
27. Kolodgie FD, Petrov A, Virmani R, Narula N, Verjans JW, Weber DK, Hartung D, Steinmetz N, Vanderheyden JL, Vannan MA, Gold HK, Reutelingsperger CP, Hofstra L, Narula J. Targeting of apoptotic macrophages and experimental atheroma with radiolabeled annexin V: a technique with potential for noninvasive imaging of vulnerable plaque. *Circulation* 2003;**108**:3134–3139.
28. Rudd JH, Myers KS, Bansilal S, Machac J, Pinto CA, Tong C, Rafique A, Hargeaves R, Farkouh M, Fuster V, Fayad ZA. Atherosclerosis inflammation imaging with ^{18}F-FDG PET: carotid, iliac, and femoral uptake reproducibility, quantification methods, and recommendations. *J Nucl Med* 2008;**49**:871–878.
29. Rudd JH, Warburton EA, Fryer TD, Jones HA, Clark JC, Antoun N, Johnstrom P, Davenport AP, Kirkpatrick PJ, Arch BN, Pickard JD, Weissberg PL. Imaging atherosclerotic plaque inflammation with [^{18}F]-fluorodeoxyglucose positron emission tomography. *Circulation* 2002;**105**:2708–2711.
30. Tawakol A, Migrino RQ, Bashian GG, Bedri S, Vermylen D, Cury RC, Yates D, LaMuraglia GM, Furie K, Houser S, Gewirtz H, Muller JE, Brady TJ, Fischman AJ. *In vivo* 18F-fluorodeoxyglucose positron emission tomography imaging provides a noninvasive measure of carotid plaque inflammation in patients. *J Am Coll Cardiol* 2006;**48**:1818–1824.
31. Tawakol A, Migrino RQ, Hoffmann U, Abbara S, Houser S, Gewirtz H, Muller JE, Brady TJ, Fischman AJ. Noninvasive *in vivo* measurement of vascular inflammation with F-18 fluorodeoxyglucose positron emission tomography. *J Nucl Cardiol* 2005;**12**:294–301.
32. Rudd JH, Myers KS, Bansilal S, Machac J, Rafique A, Farkouh M, Fuster V, Fayad ZA. (18)Fluorodeoxyglucose positron emission tomography imaging of atherosclerotic plaque inflammation is highly reproducible: implications for atherosclerosis therapy trials. *J Am Coll Cardiol* 2007;**50**:892–896.
33. Tahara N, Kai H, Yamagishi S, Mizoguchi M, Nakaura H, Ishibashi M, Kaida H, Baba K, Hayabuchi N, Imaizumi T. Vascular inflammation evaluated by [^{18}F]-fluorodeoxyglucose positron emission tomography is associated with the metabolic syndrome. *J Am Coll Cardiol* 2007;**49**:1533–1539.
34. Bural GG, Torigian DA, Chamroonrat W, Houseni M, Chen W, Basu S, Kumar R, Alavi A. FDG-PET is an effective imaging modality to detect and quantify age-related atherosclerosis in large arteries. *Eur J Nucl Med Mol Imaging* 2008;**35**:562–569.
35. Rudd JH, Myers KS, Bansilal S, Machac J, Woodward M, Fuster V, Farkouh ME, Fayad ZA. Relationships among regional arterial inflammation, calcification, risk factors, and biomarkers: a prospective fluorodeoxyglucose positron-emission tomography/computed tomography imaging study. *Circ Cardiovasc Imaging* 2009;**2**:107–115.
36. Kim TN, Kim S, Yang SJ, Yoo HJ, Seo JA, Kim SG, Kim NH, Baik SH, Choi DS, Choi KM. Vascular inflammation in patients with impaired glucose tolerance and type 2 diabetes: analysis with ^{18}F-fluorodeoxyglucose positron emission tomography. *Circ Cardiovasc Imaging* 2010;**3**:142–148.
37. Font MA, Fernandez A, Carvajal A, Gamez C, Badimon L, Slevin M, Krupinski J. Imaging of early inflammation in low-to-moderate carotid stenosis by 18-FDG-PET. *Front Biosci* 2009;**14**:3352–3360.
38. Wykrzykowska J, Lehman S, Williams G, Parker JA, Palmer MR, Varkey S, Kolodny G, Laham R. Imaging of inflamed and vulnerable plaque in coronary arteries with ^{18}F-FDG PET/CT in patients with suppression of myocardial uptake using a low-carbohydrate, high-fat preparation. *J Nucl Med* 2009;**50**:563–568.
39. Rogers IS, Nasir K, Figueroa AL, Cury RC, Hoffmann U, Vermylen DA, Brady TJ, Tawakol A. Feasibility of FDG imaging of the coronary arteries: comparison between acute coronary syndrome and stable angina. *J Am Coll Cardiol Img* 2010;**3**:388–397.
40. Tahara N, Kai H, Ishibashi M, Nakaura H, Kaida H, Baba K, Hayabuchi N, Imaizumi T. Simvastatin attenuates plaque inflammation: evaluation by fluorodeoxyglucose positron emission tomography. *J Am Coll Cardiol* 2006;**48**:1825–1831.
41. Lee SJ, On YK, Lee EJ, Choi JY, Kim BT, Lee KH. Reversal of vascular ^{18}F-FDG uptake with plasma high-density lipoprotein elevation by atherogenic risk reduction. *J Nucl Med* 2008;**49**:1277–1282.
42. Rominger A, Saam T, Wolpers S, Cyran CC, Schmidt M, Foerster S, Nikolaou K, Reiser MF, Bartenstein P, Hacker M. ^{18}F-FDG PET/CT identifies patients at risk for future vascular events in an otherwise asymptomatic cohort with neoplastic disease. *J Nucl Med* 2009;**50**:1611–1620.
43. Falk E, Sillesen H, Muntendam P, Fuster V. The high-risk plaque initiative: primary prevention of atherothrombotic events in the asymptomatic population. *Curr Atheroscler Rep* 2011;**13**:359–366.
44. Muntendam P, McCall C, Sanz J, Falk E, Fuster V. The BioImage Study: novel approaches to risk assessment in the primary prevention of atherosclerotic cardiovascular disease—study design and objectives. *Am Heart J* 2010;**160**:49.e41–57.e41.
45. Folco EJ, Sheikine Y, Rocha VZ, Christen T, Shvartz E, Sukhova GK, Di Carli MF, Libby P. Hypoxia but not inflammation augments glucose uptake in human macrophages. Implications for imaging atherosclerosis with FdG-PET. *J Am Coll Cardiol* 2011;**58**:603–614.
46. Matter CM, Wyss MT, Meier P, Spath N, von Lukowicz T, Lohmann C, Weber B, Ramirez de Molina A, Lacal JC, Ametamey SM, von Schulthess GK, Luscher TF, Kaufmann PA, Buck A. 18F-choline images murine atherosclerotic plaques *ex vivo*. *Arterioscler Thromb Vasc Biol* 2006;**26**:584–589.
47. Davies JR, Izquierdo-Garcia D, Rudd JH, Figg N, Richards HK, Bird JL, Aigbirhio FI, Davenport AP, Weissberg PL, Fryer TD, Warburton EA. FDG-PET can distinguish inflamed from non-inflamed plaque in an animal model of atherosclerosis. *Int J Cardiovasc Imaging* 2010;**26**:41–48.
48. Veenman L, Gavish M. The peripheral-type benzodiazepine receptor and the cardiovascular system. Implications for drug development. *Pharmacol Ther* 2006;**110**:503–524.
49. Braestrup C, Squires RF. Specific benzodiazepine receptors in rat brain characterized by high-affinity (3H)diazepam binding. *Proc Natl Acad Sci U S A* 1977;**74**:3805–3809.
50. Canat X, Carayon P, Bouaboula M, Cahard D, Shire D, Roque C, Le Fur G, Casellas P. Distribution profile and properties of peripheral-type benzodiazepine receptors on human hemopoietic cells. *Life Sci* 1993;**52**:107–118.
51. Canat X, Guillaumont A, Bouaboula M, Poinot-Chazel C, Derocq JM, Carayon P, LeFur G, Casellas P. Peripheral benzodiazepine receptor modulation with phagocyte differentiation. *Biochem Pharmacol* 1993;**46**:551–554.
52. Cagnin A, Kassiou M, Meikle SR, Banati RB. Positron emission tomography imaging of neuroinflammation. *Neurotherapeutics* 2007;**4**:443–452.
53. van der Laken CJ, Elzinga EH, Kropholler MA, Molthoff CF, van der Heijden JW, Maruyama K, Boellaard R, Dijkmans BA, Lammertsma AA, Voskuyl AE. Noninvasive imaging of macrophages in rheumatoid synovitis using ^{11}C-(R)-PK11195 and positron emission tomography. *Arthritis Rheum* 2008;**58**:3350–3355.

54. Fujimura Y, Hwang PM, Trout Iii H, Kozloff L, Imaizumi M, Innis RB, Fujita M. Increased peripheral benzodiazepine receptors in arterial plaque of patients with atherosclerosis: an autoradiographic study with [(^{3})H]PK 11195. *Atherosclerosis* 2008;**201**:108–111.
55. Pugliese F, Gaemperli O, Kinderlerer AR, Lamare F, Shalhoub J, Davies AH, Rimoldi OE, Mason JC, Camici PG. Imaging of vascular inflammation with [^{11}C]-PK11195 and positron emission tomography/computed tomography angiography. *J Am Coll Cardiol* 2010;**56**:653–661.
56. Lamare F, Hinz R, Gaemperli O, Pugliese F, Mason JC, Spinks T, Camici PG, Rimoldi OE. Detection and quantification of large-vessel inflammation with ^{11}C-(R)-PK11195 PET/CT. *J Nucl Med* 2010;**52**:33–39.
57. Gaemperli O, Shalhoub J, Owen DR, Lamare F, Johansson S, Fouladi N, Davies AH, Rimoldi OE, Camici PG. Imaging intraplaque inflammation in carotid atherosclerosis with 11C-PK11195 positron emission tomography/computed tomography. *Eur Heart J*; doi:10.1093/eurheartj/ehr367. Published online ahead of print 19 September 2011.
58. Gaemperli O, Boyle JJ, Rimoldi OE, Mason JC, Camici PG. Molecular imaging of vascular inflammation. *Eur J Nucl Med Mol Imaging* 2010;**37**:1236.
59. Briard E, Zoghbi SS, Simeon FG, Imaizumi M, Gourley JP, Shetty HU, Lu S, Fujita M, Innis RB, Pike VW. Single-step high-yield radiosynthesis and evaluation of a sensitive 18F-labeled ligand for imaging brain peripheral benzodiazepine receptors with PET. *J Med Chem* 2009;**52**:688–699.
60. Pundziute G, Schuijf JD, Jukema JW, Decramer I, Sarno G, Vanhoenacker PK, Reiber JH, Schalij MJ, Wijns W, Bax JJ. Head-to-head comparison of coronary plaque evaluation between multislice computed tomography and intravascular ultrasound radiofrequency data analysis. *J Am Coll Cardiol Intv* 2008;**1**:176–182.
61. Halliburton SS, Schoenhagen P, Nair A, Stillman A, Lieber M, Murat Tuzcu E, Geoffrey Vince D, White RD. Contrast enhancement of coronary atherosclerotic plaque: a high-resolution, multidetector-row computed tomography study of pressure-perfused, human *ex vivo* coronary arteries. *Coron Artery Dis* 2006;**17**:553–560.
62. Kashiwagi M, Tanaka A, Kitabata H, Tsujioka H, Kataiwa H, Komukai K, Tanimoto T, Takemoto K, Takarada S, Kubo T, Hirata K, Nakamura N, Mizukoshi M, Imanishi T, Akasaka T. Feasibility of noninvasive assessment of thin-cap fibroatheroma by multidetector computed tomography. *J Am Coll Cardiol Img* 2009;**2**:1412–1419.
63. Voros S, Rinehart S, Qian Z, Joshi P, Vazquez G, Fischer C, Belur P, Hulten E, Villines TC. Coronary atherosclerosis imaging by coronary CT angiography: current status, correlation with intravascular interrogation and meta-analysis. *J Am Coll Cardiol Img* 2011;**4**:537–548.
64. Hoffmann U, Moselewski F, Nieman K, Jang IK, Ferencik M, Rahman AM, Cury RC, Abbara S, Joneidi-Jafari H, Achenbach S, Brady TJ. Noninvasive assessment of plaque morphology and composition in culprit and stable lesions in acute coronary syndrome and stable lesions in stable angina by multidetector computed tomography. *J Am Coll Cardiol* 2006;**47**:1655–1662.
65. Motoyama S, Kondo T, Sarai M, Sugiura A, Harigaya H, Sato T, Inoue K, Okumura M, Ishii J, Anno H, Virmani R, Ozaki Y, Hishida H, Narula J. Multislice computed tomographic characteristics of coronary lesions in acute coronary syndromes. *J Am Coll Cardiol* 2007;**50**:319–326.
66. Motoyama S, Sarai M, Harigaya H, Anno H, Inoue K, Hara T, Naruse H, Ishii J, Hishida H, Wong ND, Virmani R, Kondo T, Ozaki Y, Narula J. Computed tomographic angiography characteristics of atherosclerotic plaques subsequently resulting in acute coronary syndrome. *J Am Coll Cardiol* 2009;**54**:49–57.
67. Hyafil F, Cornily JC, Feig JE, Gordon R, Vucic E, Amirbekian V, Fisher EA, Fuster V, Feldman LJ, Fayad ZA. Noninvasive detection of macrophages using a nanoparticulate contrast agent for computed tomography. *Nat Med* 2007;**13**:636–641.
68. Hyafil F, Cornily JC, Rudd JH, Machac J, Feldman LJ, Fayad ZA. Quantification of inflammation within rabbit atherosclerotic plaques using the macrophage-specific CT contrast agent N1177: a comparison with 18F-FDG PET/CT and histology. *J Nucl Med* 2009;**50**:959–965.
69. Weissleder R, Mahmood U. Molecular imaging. *Radiology* 2001;**219**:316–333.
70. Cormode DP, Roessl E, Thran A, Skajaa T, Gordon RE, Schlomka JP, Fuster V, Fisher EA, Mulder WJ, Proksa R, Fayad ZA. Atherosclerotic plaque composition: analysis with multicolor CT and targeted gold nanoparticles. *Radiology* 2010;**256**:774–782.
71. Hatsukami TS, Yuan C. MRI in the early identification and classification of high-risk atherosclerotic carotid plaques. *Imaging Med* 2010;**2**:63–75.
72. van den Bouwhuijsen QJ, Vernooij MW, Hofman A, Krestin GP, van der Lugt A, Witteman JC. Determinants of magnetic resonance imaging detected carotid plaque components: the Rotterdam Study. *Eur Heart J* 2012;**33**:221–229.
73. Mitsumori LM, Hatsukami TS, Ferguson MS, Kerwin WS, Cai J, Yuan C. *In vivo* accuracy of multisequence MR imaging for identifying unstable fibrous caps in advanced human carotid plaques. *J Magn Reson Imaging* 2003;**17**:410–420.
74. Cai J, Hatsukami TS, Ferguson MS, Kerwin WS, Saam T, Chu B, Takaya N, Polissar NL, Yuan C. *In vivo* quantitative measurement of intact fibrous cap and lipid-rich necrotic core size in atherosclerotic carotid plaque: comparison of high-resolution, contrast-enhanced magnetic resonance imaging and histology. *Circulation* 2005;**112**:3437–3444.
75. Takaya N, Cai J, Ferguson MS, Yarnykh VL, Chu B, Saam T, Polissar NL, Sherwood J, Cury RC, Anders RJ, Broschat KO, Hinton D, Furie KL, Hatsukami TS, Yuan C. Intra- and interreader reproducibility of magnetic resonance imaging for quantifying the lipid-rich necrotic core is improved with gadolinium contrast enhancement. *JMRI* 2006;**24**:203–210.
76. Young VE, Patterson AJ, Sadat U, Bowden DJ, Graves MJ, Tang TY, Priest AN, Skepper JN, Kirkpatrick PJ, Gillard JH. Diffusion-weighted magnetic resonance imaging for the detection of lipid-rich necrotic core in carotid atheroma *in vivo*. *Neuroradiology* 2010;**52**:929–936.
77. Yuan C, Mitsumori LM, Ferguson MS, Polissar NL, Echelard D, Ortiz G, Small R, Davies JW, Kerwin WS, Hatsukami TS. *In vivo* accuracy of multispectral magnetic resonance imaging for identifying lipid-rich necrotic cores and intraplaque hemorrhage in advanced human carotid plaques. *Circulation* 2001;**104**:2051–2056.
78. Takaya N, Yuan C, Chu B, Saam T, Polissar NL, Jarvik GP, Isaac C, McDonough J, Natiello C, Small R, Ferguson MS, Hatsukami TS. Presence of intraplaque hemorrhage stimulates progression of carotid atherosclerotic plaques: a high-resolution magnetic resonance imaging study. *Circulation* 2005;**111**:2768–2775.
79. Altaf N, Goode SD, Beech A, Gladman JR, Morgan PS, MacSweeney ST, Auer DP. Plaque hemorrhage is a marker of thromboembolic activity in patients with symptomatic carotid disease. *Radiology* 2011;**258**:538–545.
80. Kerwin W, Hooker A, Spilker M, Vicini P, Ferguson M, Hatsukami T, Yuan C. Quantitative magnetic resonance imaging analysis of neovasculature volume in carotid atherosclerotic plaque. *Circulation* 2003;**107**:851–856.
81. Sirol M, Moreno PR, Purushothaman KR, Vucic E, Amirbekian V, Weinmann HJ, Muntner P, Fuster V, Fayad ZA. Increased neovascularization in advanced lipid-rich atherosclerotic lesions detected by gadofluorine-M-enhanced MRI: implications for plaque vulnerability. *Circ Cardiovasc Imaging* 2009;**2**:391–396.
82. Kerwin WS. Noninvasive imaging of plaque inflammation: role of contrast-enhanced MRI. *J Am Coll Cardiol Img* 2010;**3**:1136–1138.
83. Tang T, Howarth SP, Miller SR, Trivedi R, Graves MJ, King-Im JU, Li ZY, Brown AP, Kirkpatrick PJ, Gaunt ME, Gillard JH. Assessment of inflammatory burden contralateral to the symptomatic carotid stenosis using high-resolution ultrasmall, superparamagnetic iron oxide-enhanced MRI. *Stroke* 2006;**37**:2266–2270.
84. Trivedi RA, Mallawarachi C, U-King-Im JM, Graves MJ, Horsley J, Goddard MJ, Brown A, Wang L, Kirkpatrick PJ, Brown J, Gillard JH. Identifying inflamed carotid plaques using *in vivo* USPIO-enhanced MR imaging to label plaque macrophages. *Arterioscler Thromb Vasc Biol* 2006;**26**:1601–1606.
85. Cury RC, Houser SL, Furie KL, Stone JR, Ogilvy CS, Sherwood JB, Muller JE, Brady TJ, Hinton DP. Vulnerable plaque detection by 3.0 tesla magnetic resonance imaging. *Invest Radiol* 2006;**41**:112–115.
86. Cheng C, Tempel D, van Haperen R, van der Baan A, Grosveld F, Daemen MJ, Krams R, de Crom R. Atherosclerotic lesion size and vulnerability are determined by patterns of fluid shear stress. *Circulation* 2006;**113**:2744–2753.
87. Chatzizisis YS, Coskun AU, Jonas M, Edelman ER, Feldman CL, Stone PH. Role of endothelial shear stress in the natural history of coronary atherosclerosis and vascular remodeling: molecular, cellular, and vascular behavior. *J Am Coll Cardiol* 2007;**49**:2379–2393.
88. Caro CG. Discovery of the role of wall shear in atherosclerosis. *Arteriosc Thromb Vasc Biol* 2009;**29**:158–161.
89. Tang D, Teng Z, Canton G, Yang C, Ferguson M, Huang X, Zheng J, Woodard PK, Yuan C. Sites of rupture in human atherosclerotic carotid plaques are associated with high structural stresses: an *in vivo* MRI-based 3D fluid-structure interaction study. *Stroke* 2009;**40**:3258–3263.
90. Sadat U, Li ZY, Young VE, Graves MJ, Boyle JR, Warburton EA, Varty K, O'Brien E, Gillard JH. Finite element analysis of vulnerable atherosclerotic plaques: a comparison of mechanical stresses within carotid plaques of acute and recently symptomatic patients with carotid artery disease. *J Neurol Neurosurg Psychiatry* 2010;**81**:286–289.
91. Sadat U, Teng Z, Young VE, Graves MJ, Gaunt ME, Gillard JH. High-resolution magnetic resonance imaging-based biomechanical stress analysis of carotid atheroma: a comparison of single transient ischaemic attack, recurrent transient ischaemic attacks, non-disabling stroke and asymptomatic patient groups. *Eur J Vasc Endovasc Surg* 2011;**41**:83–90.
92. Saam T, Hatsukami TS, Takaya N, Chu B, Underhill H, Kerwin WS, Cai J, Ferguson MS, Yuan C. The vulnerable, or high-risk, atherosclerotic plaque: noninvasive MR imaging for characterization and assessment. *Radiology* 2007;**244**:64–77.
93. Demarco JK, Ota H, Underhill HR, Zhu DC, Reeves MJ, Potchen MJ, Majid A, Collar A, Talsma JA, Potru S, Oikawa M, Dong L, Zhao X, Yarnykh VL,

Yuan C. MR carotid plaque imaging and contrast-enhanced MR angiography identifies lesions associated with recent ipsilateral thromboembolic symptoms: an *in vivo* study at 3T. *AJNR Am J Neuroradiol* 2010;**31**:1395–1402.
94. Yuan C, Zhang SX, Polissar NL, Echelard D, Ortiz G, Davis JW, Ellington E, Ferguson MS, Hatsukami TS. Identification of fibrous cap rupture with magnetic resonance imaging is highly associated with recent transient ischemic attack or stroke. *Circulation* 2002;**105**:181–185.
95. Takaya N, Yuan C, Chu B, Saam T, Underhill H, Cai J, Tran N, Polissar NL, Isaac C, Ferguson MS, Garden GA, Cramer SC, Maravilla KR, Hashimoto B, Hatsukami TS. Association between carotid plaque characteristics and subsequent ischemic cerebrovascular events: a prospective assessment with MRI—initial results. *Stroke* 2006;**37**:818–823.
96. Kerwin WS, O'Brien KD, Ferguson MS, Polissar N, Hatsukami TS, Yuan C. Inflammation in carotid atherosclerotic plaque: a dynamic contrast-enhanced MR imaging study. *Radiology* 2006;**241**:459–468.
97. Jaffer FA, Nahrendorf M, Sosnovik D, Kelly KA, Aikawa E, Weissleder R. Cellular imaging of inflammation in atherosclerosis using magnetofluorescent nanomaterials. *Molec Imag* 2006;**5**:85–92.
98. Mani V, Briley-Saebo KC, Hyafil F, Fayad ZA. Feasibility of *in vivo* identification of endogenous ferritin with positive contrast MRI in rabbit carotid crush injury using GRASP. *Magn Reson Med* 2006;**56**:1096–1106.
99. Makowski MR, Varma G, Wiethoff AJ, Smith A, Mattock K, Jansen CH, Warley A, Taupitz M, Schaeffter T, Botnar RM. Noninvasive assessment of atherosclerotic plaque progression in ApoE-/- mice using susceptibility gradient mapping. *Circ Cardiovasc Imaging* 2011;**4**:295–303.
100. Tang TY, Patterson AJ, Miller SR, Graves MJ, Howarth SP, U-King-Im JM, Li ZY, Sadat U, Young VE, Walsh SR, Boyle JR, Gaunt ME, Gillard JH. Temporal dependence of *in vivo* USPIO-enhanced MRI signal changes in human carotid atheromatous plaques. *Neuroradiology* 2009;**51**:457–465.
101. Tang TY, Howarth SP, Miller SR, Graves MJ, Patterson AJ, U-King-Im JM, Li ZY, Walsh SR, Brown AP, Kirkpatrick PJ, Warburton EA, Hayes PD, Varty K, Boyle JR, Gaunt ME, Zalewski A, Gillard JH. The ATHEROMA (Atorvastatin Therapy: Effects on Reduction of Macrophage Activity) Study. Evaluation using ultrasmall superparamagnetic iron oxide-enhanced magnetic resonance imaging in carotid disease. *J Am Coll Cardiol* 2009;**53**:2039–2050.
102. Virmani R, Kolodgie FD, Burke AP, Finn AV, Gold HK, Tulenko TN, Wrenn SP, Narula J. Atherosclerotic plaque progression and vulnerability to rupture: angiogenesis as a source of intraplaque hemorrhage. *Arterioscler Thromb Vasc Biol* 2005; **25**:2054–2061.
103. Davies MJ, Thomas AC. Plaque fissuring—the cause of acute myocardial infarction, sudden ischemic death, and crescendo angina. *British Heart J* 1985;**53**: 363–373.
104. Moody AR, Murphy RE, Morgan PS, Martel AL, Delay GS, Allder S, MacSweeney ST, Tennant WG, Gladman J, Lowe J, Hunt BJ. Characterization of complicated carotid plaque with magnetic resonance direct thrombus imaging in patients with cerebral ischemia. *Circulation* 2003;**107**:3047–3052.
105. Saam T, Cai J, Ma L, Cai YQ, Ferguson MS, Polissar NL, Hatsukami TS, Yuan C. Comparison of symptomatic and asymptomatic atherosclerotic carotid plaque features with *in vivo* MR imaging. *Radiology* 2006;**240**:464–472.
106. Singh N, Moody AR, Gladstone DJ, Leung G, Ravikumar R, Zhan J, Maggisano R. Moderate carotid artery stenosis: MR imaging-depicted intraplaque hemorrhage predicts risk of cerebrovascular ischemic events in asymptomatic men. *Radiology* 2009;**252**:502–508.
107. Zhao X, Underhill HR, Zhao Q, Cai J, Li F, Oikawa M, Dong L, Ota H, Hatsukami TS, Chu B, Yuan C. Discriminating carotid atherosclerotic lesion severity by luminal stenosis and plaque burden. *Stroke* 2011;**42**:347–353.
108. Maintz D, Ozgun M, Hoffmeier A, Fischbach R, Kim WY, Stuber M, Manning WJ, Heindel W, Botnar RM. Selective coronary artery plaque visualization and differentiation by contrast-enhanced inversion prepared MRI. *Eur Heart J* 2006;**27**: 1732–1736.
109. Lindner JR. Molecular imaging of cardiovascular disease with contrast-enhanced ultrasonography. *Nat Rev Cardiol* 2009;**6**:475–481.
110. Villanueva FS, Wagner WR. Ultrasound molecular imaging of cardiovascular disease. *Nat Clin Pract Cardiovasc Med* 2008;**5**(Suppl. 2):S26–S32.
111. Coli S, Magnoni M, Sangiorgi G, Marrocco-Trischitta MM, Melisurgo G, Mauriello A, Spagnoli L, Chiesa R, Cianflone D, Maseri A. Contrast-enhanced ultrasound imaging of intraplaque neovascularization in carotid arteries: correlation with histology and plaque echogenicity. *J Am Coll Cardiol* 2008;**52**:223–230.
112. Magnoni M, Coli S, Cianflone D. A surprise behind the dark. *Eur J Echocardiogr* 2009;**10**:887–888.